J. Plasma Fusion Res. SERIES, Vol. 2 (1999) 363–367

Structure of Multi-Dimensional Soliton and Generation of Caviton in the Nonlinear Beam-Plasma System

MORI Ichiro, MORIMOTO Toshifumi[1], KAWAKAMI Retsuo and TOMINAGA Kikuo
Faculty of Engineering The University of Tokushima, Minami-josanjima 770 Tokushima Japan
[1]Takuma Radio Technical College, Kohda, Takuma, 761-11, Kagawa, Japan

(Received: 8 December 1998 / Accepted: 24 February 1999)

Abstract

Results of experimental analysis with respect to the mechanism for generation of soliton, and also that of the cavitons are discussed. The appearance of the solitons coincide actually with the ion waves (or the cavitons). A new theory is obtained by using renormalization technique with Gaussian type Green's function. Our theory shows that the beam electron can not emit the elementary excitation (soliton) by itself, but can emit by coherent interaction between electrons through intermediation of the elementary excitation (phonon), under the presence of ions.

Keywords:

soliton, caviton, beam-plasma

1. Introduction

One dimensional envelope solitons appeared in the field of applied or plasma physics, which are rather idealized one, has been almost analyzed and completed. In the actual experimental plasma, however, soliton is multi-dimensional (three dimensional) and restricted by boundary such as density gradient or magnetic field gradient. In experimental stand point, these non-homogenity play a role of driving force to make the soliton. In this paper, we discuss the ground for generation of soliton in the mirror magnetic field.

2. Experiments

2.1. Plasma density

We used the field, 80Gauss in center and mirror ratio of 1.4. A stainless vessel for plasma region is 16cm in diameter and 42cm in length. The region is initially evacuated to 10^{-6}Torr and is fed with argon gas from 10^{-4} to 7×10^{-4}Torr. A beam of 8mm in diameter, 1.9keV–18mA, is injected into plasma. Any plasma density of 10^{14}~5×10^{15}m^{-3} in center is possible.

Figure 1 shows the spatial plasma density, n_e, and also the magnetic field density distribution. The plasma density was measured by probe and calibrated initially by micro-wave experiment with small horn at center position. The scale of *5* on vertical axis corresponds to the density of 1.5×10^{15}m^{-3}. At the gas pressure of $\simeq 2.1 \times 10^{-4}$Torr, the plasma density increases suddenly by ionization of large amplitude solitary wave, we call this stage as *second stage*. The solitary wave appears as burst with time width 150~500nsec having an envelope of hyperbolic secant curve at low gas pressure, whose carrier frequency is $\simeq$ 400MHz. Phase of the carrier is confirmed to be continuous with 2GHz oscilloscope. The solitary waves are constantly generated as an intermittent burst in suspended time of every 4≃8μsec. It is also found that the density cavities are formed by pressure of the successive bursts and by retarded responce of ions, as shown on the curve of gas pressure 2.2×10^{-4} at the position 20~25cm measured from beam entrance.

Corresponding author's e-mail: mori@ee.tokushima-u.ac.jp

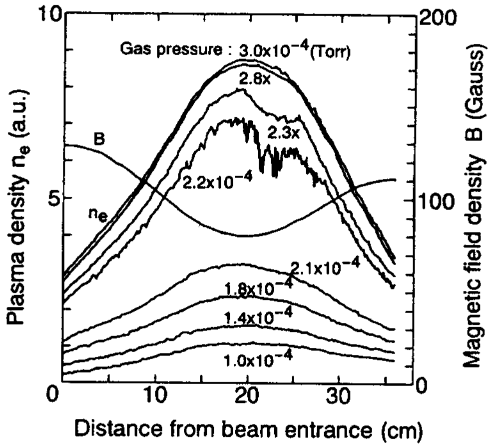

Fig. 1 Spatial distributions of the plasma density and the magnetic field density are presented. The scale of *5* on vertical axis corresponds to the density of 1.5 $\times 10^{15}$m^{-3}. Pressure balance: $(\varepsilon \boldsymbol{E}^2/2) + (\mu \boldsymbol{H}^2/2) + p =$ const. is shown, where the p, $\boldsymbol{E}$ are the plasma pressure, electric field by soliton, respectively.

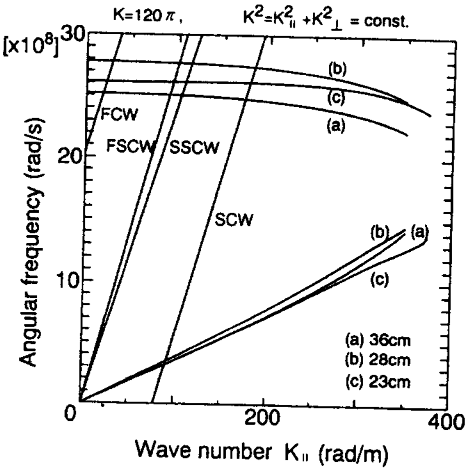

Fig. 2 Examples of dispersion relation for hybrid wave at several point are shown. The burst-wave generation by non-convective interaction between the wave branch (a) and the beam's space charge wave (SSCW) can be expected.

2.2. Dispersion relation

From the plasma density and the magnetic field density mentioned above, one can obtain dispersion relation of hybrid wave at each point, then an original dispersion relation [1] is asymptotically expanded and get finally the following equation:

$$
\begin{aligned}
\boldsymbol{k}_{\parallel}^2 + \boldsymbol{k}_{\perp}^2 - \sum_{\alpha} \Bigg[& \frac{\omega_{p\alpha}^2}{\omega^2} \boldsymbol{k}_{\parallel}^2 + \frac{3}{2} \cdot \frac{\omega_{p\alpha}^2 \boldsymbol{k}_{\parallel}^4 \boldsymbol{v}_{T\parallel}^2}{\omega^4} \\
& - \frac{1}{2} \cdot \frac{\omega_{p\alpha}^2 \boldsymbol{k}_{\parallel}^2 \boldsymbol{k}_{\perp}^2 \boldsymbol{v}_{T\perp}^2}{\omega^2 \omega_{c\alpha}^2} \\
& + \frac{1}{2} \cdot \frac{\boldsymbol{k}_{\parallel}^2 \boldsymbol{k}_{\perp}^2 \boldsymbol{v}_{T\perp}^2 (\omega^2 + \omega_{c\alpha}^2) \omega_{p\alpha}^2}{(\omega^2 - \omega_{c\alpha}^2) \omega_{c\alpha}^2} \\
& + \frac{\omega_{p\alpha}^2 \boldsymbol{k}_{\perp}^2}{\omega^2 - \omega_{c\alpha}^2} - \frac{1}{2} \cdot \frac{\omega_{p\alpha}^2 \boldsymbol{k}_{\perp}^4 \boldsymbol{v}_{T\perp}^2}{(\omega^2 - \omega_{c\alpha}^2) \omega_{c\alpha}^2} \\
& + \frac{1}{2} \cdot \frac{\boldsymbol{k}_{\parallel}^2 \boldsymbol{k}_{\perp}^2 \boldsymbol{v}_{T\parallel}^2 (3\omega^2 - \omega_{c\alpha}^2) \omega_{p\alpha}^2}{(\omega^2 - \omega_{c\alpha}^2)^3} \\
& + \frac{1}{2} \cdot \frac{\boldsymbol{k}_{\perp}^4 \boldsymbol{v}_{T\perp}^2 \omega_{p\alpha}^2}{(\omega^2 - 4\omega_{c\alpha}^2) \omega_{c\alpha}^2} \Bigg] = 0 .
\end{aligned}
$$

Thus we obtained a twelveth order algebraic equation for ω, and solved ω for a known set of $(\boldsymbol{k}_{\parallel}, \boldsymbol{k}_{\perp})$. We assumed that the hybrid wave propagates in such a way that energy, $\hbar\omega$, and momentum, $\hbar \boldsymbol{k}$, of the elementary excitation were conserved everywhere, then the requirements $\omega =$ const., $\boldsymbol{k}_{\parallel}^2 + \boldsymbol{k}_{\perp}^2 = \boldsymbol{k}^2 =$ const. were used.

Figure 2 represents the dispersion at different position, where the two wave groups, upper hybrid wave and lower hybrid wave are seen in the same sign: (a), (b), (c). In the figure, beam waves such as *slow space charge wave* (SSCW), *fast space charge wave* (FSCW), *slow cyclotron wave* (SCW), *fast cyclotron wave* (FCW) are presented.

2.3. Non-convective instability and group velocity dispersion

In beam-plasma system, wave generation by non-convective interaction between the upper hybrid wave and the beam's slow space charge wave (SSCW) at the intersecting point of both dispersion curves, can be surely expected. In fig.2, for example, the intersecting point between the curve (a) and the SSCW is given by $\{\boldsymbol{k}_{\parallel} = 103.3$ (rad/m), $\omega = 2.505 \times 10^9$ (rad/sec)$\}$, then the generating backward wave at 36cm point can propagate to 23cm point by decreasing $\boldsymbol{k}_{\perp}$ and increasing $\boldsymbol{k}_{\parallel}$ by the restrictions $\omega = 2.505 \times 10^9 \simeq 400$MHz = constant and $|\boldsymbol{k}| = 120\pi =$ constant.

Figure 3 shows dispersion relation at 36cm point.

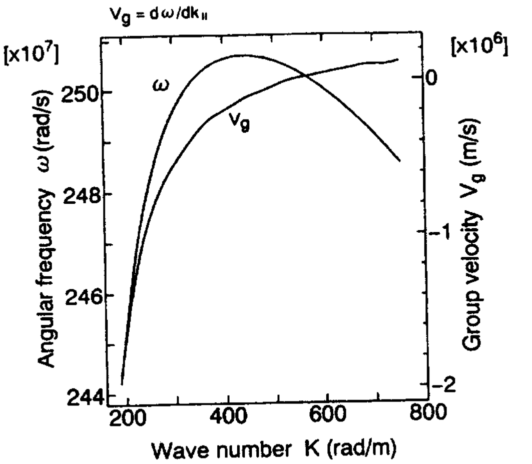

Fig. 3 Group velocity dispersion at 36cm point is presented. The region of the negative group velocity shows abnormal dispersion and the burst-wave generation is expected as in the optical solitons in fibers. We assumed that the momentum of an elementary excitation, $\hbar \boldsymbol{k}$, is conserved at any position.

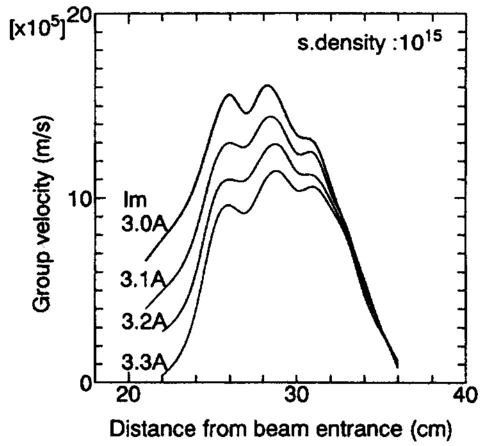

Fig. 4 Calculated group velocities from the data of fig.1 at which main field current, I_m, is 3A, are presented as the function of position. The generated wave at 36cm point propagate oppositely against the beam, and their group velocity lessen near the position of cavities. Possible mechanism of energy accumulation of the soliton may thus be occured by this slowing down.

The horizontal axis is $|\boldsymbol{k}|$ and not a $\boldsymbol{k}_\parallel$, because the $\boldsymbol{k}_\parallel$ is slowly increasing function with ω and decided only by resonance condition of the beam: $\omega - \boldsymbol{k}_\parallel \cdot \boldsymbol{v}_\parallel - \mathrm{Im}\Sigma_\alpha = 0$, where $\boldsymbol{v}_\parallel$ is the beam velocity and the Σ_α is a resonance broadening. The ω has maximum at $|\boldsymbol{k}| = 440$ (rad/m). For the large $|\boldsymbol{k}|$, group velocity, $\partial\omega/\partial|\boldsymbol{k}|$, changes its direction. Backward group velocity defined by $\boldsymbol{v}_g = \partial\omega/\partial\boldsymbol{k}_\parallel$, is also presented in the figure and some shift of the zero-group-velocity point compared with the former owing to $\boldsymbol{k}_\perp$, is seen. The fact that the large wave length is related to the large $\boldsymbol{v}_g$, is quite similar to the propagation of optical soliton in a fiber, therefore, the large wave length region corresponds to negative group velocity dispersion and medium has *abnormal dispersion*. At the 36cm point, plasma frequency is smaller than the cyclotron frequency, $\omega_{pe} < \omega_{ce}$, while at 23cm point, opposite relation is held, $\omega_{pe} > \omega_{ce}$. It seems that the higher density region is suitable to *normal dispersion*.

Figure 4 represents the group velocities at each point. The parameter Im = 3.0A~3.3A is a main magnetic field current. The group velocity increases at $\simeq$36cm point and decreases at $\simeq$23cm point. This result fits the fact that any waves can not enter the high density region except the digging caviton by soliton pressure. Thus we can justify the many experimental results including soliton.

3. The Nonlinear Theory

3.1. Soliton generation

Weexamine to describe an emissinof a solitary wave with the electron beam by using *the renormalization technique* which was developed by Al'tshul, Karpmann [2], Dupree [3], Weinstock [4], Kono, Ichikawa [5]. For the soliton, one must put emphasis on coherent interaction of same wave number, i.e., $\boldsymbol{k}_1 = \boldsymbol{k}$, while the theory of Weinstock dealt with the case $|\boldsymbol{k}_1| \gg |\boldsymbol{k}|$ and if we use the case $\boldsymbol{k}_1 = \boldsymbol{k}$ in the discussion of Kono, Ichikawa, their diffusion coefficient degenerate to that of the *quasi-linear theory*. Then we used a Gausian-type Green's function that was proposed initially by Horton [6] and define a diffusion tensor D_{ij} instead of scalar function D, then the Green function is described as:

$$G_\alpha(\boldsymbol{k},\boldsymbol{v},t;\boldsymbol{k}',\boldsymbol{v}',t') = -\mathrm{i}\left\{\frac{4\pi}{\boldsymbol{k}^2}\boldsymbol{k}_i\boldsymbol{k}_j\boldsymbol{D}_{ij}(\boldsymbol{k},\boldsymbol{v})t\right\}^{-\frac{3}{2}}$$

$$\cdot\exp\left[-\frac{\boldsymbol{k}_i(\boldsymbol{v}-\boldsymbol{v}')_i\boldsymbol{k}_j(\boldsymbol{v}-\boldsymbol{v}')_j}{4\boldsymbol{k}_i\boldsymbol{k}_j\boldsymbol{D}_{ij}(\boldsymbol{k},\boldsymbol{v})t} - \frac{\boldsymbol{k}_i\boldsymbol{k}_j\boldsymbol{D}_{ij}(\boldsymbol{k},\boldsymbol{v})}{12}t^3\right.$$

$$\left.-\frac{\mathrm{i}}{2}\boldsymbol{k}\cdot(\boldsymbol{v}+\boldsymbol{v}')t\right]\delta_{\boldsymbol{k},\boldsymbol{k}'}$$

Fourier transformation of the above Geen's function becomes:

$$G(\boldsymbol{k}, \boldsymbol{v}, \omega; \boldsymbol{k}', \boldsymbol{v}', \omega') = -2\mathrm{i}\,\{4\pi(\frac{\boldsymbol{k}_i \boldsymbol{k}_j}{\boldsymbol{k}^2}) \cdot D_{ij}(\boldsymbol{k}, \boldsymbol{v})\}^{-\frac{3}{2}} \sum_{m=1}^{\infty} \frac{(-b)^m}{m!} \{\frac{a}{\mathrm{i}(-\omega + c)}\}^{\frac{3m}{2} - \frac{1}{4}} \cdot K_{3m-\frac{1}{2}}\{2\sqrt{\mathrm{i}\,a(-\omega + c)}\}\, \delta_{\boldsymbol{k},\boldsymbol{k}'}\, \delta_{\omega,\omega'} \quad (1)$$

$$a = \frac{\boldsymbol{k}_i (\boldsymbol{v} - \boldsymbol{v}')_i \boldsymbol{k}_j (\boldsymbol{v} - \boldsymbol{v}')_j}{4\boldsymbol{k}_i \boldsymbol{k}_j \cdot D_{ij}(\boldsymbol{k}, \boldsymbol{v})},$$

$$b = \frac{\boldsymbol{k}_i \boldsymbol{k}_j \cdot D_{ij}(\boldsymbol{k}, \boldsymbol{v})}{12}, \quad c = \boldsymbol{k} \cdot \boldsymbol{v} - \mathrm{i}\,\Sigma_\alpha,$$

where the function $K_{3m-\frac{1}{2}}(x)$ is the modified Bessel function and $m = 0$ term is very important and $K_{-\frac{1}{2}}(x) = K_{\frac{1}{2}}(x) = \sqrt{\pi/(2x)}\cdot\exp(-x)$. The terms $m \neq 0$ areproportional to $\boldsymbol{k}^{2m}$ then they vanish when we consider the limit $\boldsymbol{k} \to 0$. For the quantity $\boldsymbol{k}_i\boldsymbol{k}_j D_{ij}/\boldsymbol{k}^2$, we use D_{ij} simply as scalar since the $\boldsymbol{k}_i\boldsymbol{k}_j/\boldsymbol{k}^2$ is O(1), then

$$G_\alpha(m=0) = -\frac{\mathrm{i}}{4\pi D_{ij}} \cdot \frac{1}{|\boldsymbol{v} - \boldsymbol{v}'|} \cdot \exp\left(-\frac{|\boldsymbol{v} - \boldsymbol{v}'|}{\sqrt{D_{ij}}} \cdot \sqrt{\mathrm{i}(-\omega + c)}\right). \quad (1')$$

We denote that $f_\alpha^{(0)}(\boldsymbol{k}', \boldsymbol{v}', \omega')$, $\Sigma_\alpha(\boldsymbol{k}, \boldsymbol{v}, \omega)$ are the initial beam distribution and the collision frequency between electrons and the elementary excitations or self-energy term respectively.

$$D_{ij}(\boldsymbol{k}, \boldsymbol{v}) = (\frac{e_\alpha}{m_\alpha})^2 \sum_{k_1} \int \frac{\mathrm{d}\omega_1}{2\pi} \frac{\boldsymbol{k}_{1i} \boldsymbol{k}_{1j}}{\boldsymbol{k}_1^2} |\boldsymbol{E}(\boldsymbol{k}_1, \omega_1)|^2 G_\alpha(\boldsymbol{k} - \boldsymbol{k}_1, \boldsymbol{v}, \boldsymbol{k}\cdot\boldsymbol{v} - \omega_1; \boldsymbol{k}', \boldsymbol{v}', \omega'), \quad (2)$$

$$\boldsymbol{E}(\boldsymbol{k}, \omega) = -\sum_\alpha \frac{e_\alpha}{\varepsilon_0} \cdot \frac{\mathrm{i}\boldsymbol{k}}{\boldsymbol{k}^2} \int \mathrm{d}\boldsymbol{v} \int \mathrm{d}\boldsymbol{v}' \int \frac{\mathrm{d}\boldsymbol{k}'}{(2\pi)^3} G_\alpha(\boldsymbol{k}, \boldsymbol{v}, \omega; \boldsymbol{k}', \boldsymbol{v}', \omega') \cdot f_\alpha^{(0)}(\boldsymbol{k}', \boldsymbol{v}', \omega'), \quad (3)$$

$$f_\alpha(\boldsymbol{k}, \boldsymbol{v}, \omega) = \int \mathrm{d}\boldsymbol{v}' G_\alpha(\boldsymbol{k}, \boldsymbol{v}, \omega; \boldsymbol{k}', \boldsymbol{v}', \omega') \cdot f_\alpha^{(0)}(\boldsymbol{k}', \boldsymbol{v}', \omega'), \quad (4)$$

$$\Sigma_\alpha(\boldsymbol{k}, \boldsymbol{v}, \omega) = (\frac{e_\alpha}{m_\alpha})^2 \sum_{k_1} \int \frac{\mathrm{d}\omega_1}{2\pi} \boldsymbol{E}(\boldsymbol{k}_1, \omega_1) \cdot \frac{\partial}{\partial \boldsymbol{v}} \{G_\alpha(\boldsymbol{k} - \boldsymbol{k}_1, \boldsymbol{v}, \boldsymbol{k}\cdot\boldsymbol{v} - \omega_1) \cdot \boldsymbol{E}(-\boldsymbol{k}_1, -\omega_1) \cdot \frac{\partial}{\partial \boldsymbol{v}}\}. \quad (5)$$

The eqs. (1)~(5) construct a set of fundamental equation to analyze the soliton emission. The soliton comes from 3rd order nonlinear, while the diffusion coefficient in velocity space, D_{ij}, and the self energy part, Σ_α, have 2nd order nonlinear since they include a factor: $|\boldsymbol{E}(\boldsymbol{k}_1, \omega_1)|^2 \cdot G_\alpha(\boldsymbol{k} - \boldsymbol{k}_1, \boldsymbol{v}, \boldsymbol{k}\cdot\boldsymbol{v} - i\Sigma_\alpha - \omega_1)$. For the 3rd order solution, it is sufficient to substitute the D_{ij} or the Σ_α for old quantities and get new Green's function. Thus the $\boldsymbol{E}(\boldsymbol{k}, \omega), f^\alpha(\boldsymbol{k}, \boldsymbol{v}, \omega)$ are obtained in 3rd order, howeverb the soliton comes also from coherent interaction, $\boldsymbol{k}_1 = \boldsymbol{k}$, then the limits $\boldsymbol{k}_1 \to \boldsymbol{k}$, and $\omega_1 \to \boldsymbol{k}\cdot\boldsymbol{v}$ must be taken. The Green's function eq. (1') is sternly normal and regular and not vanish even if at $\boldsymbol{k} = 0$ in contrast to the *linear* case.

To solve the 3rd order solutions, we used only m = 0-th term and assumed firstly that $|\boldsymbol{E}(\boldsymbol{k}_1, \omega_1)|^2 = |\boldsymbol{E}|^2 =$ const. in the expressions of $D_{ij}(\boldsymbol{k}, \boldsymbol{v})$, and $\Sigma_\alpha(\boldsymbol{k}, \boldsymbol{v}, \omega)$, then the $\boldsymbol{E}(\boldsymbol{k}, t), f^\alpha(\boldsymbol{k}, \boldsymbol{v}, t)$ are solved as initial value problems through inverse transformation. Results would be presented elsewhere [7].

3.2. Interaction with ions & anomalous collision

The quantity $|\boldsymbol{E}(\boldsymbol{k}_1, \omega_1)|^2 \cdot G_\alpha(\boldsymbol{k} - \boldsymbol{k}_1, \boldsymbol{v}, \boldsymbol{k}\cdot\boldsymbol{v} - \mathrm{i}\Sigma_\alpha - \omega_1)$ means that two electrons which have $(\omega, \boldsymbol{k})$ and $(-\omega_1, -\boldsymbol{k}_1)$, interact trough exchanging the elementary excitations (phonons) munder the presence of ions, since the coherent interaction brings about an increase of electron's $\boldsymbol{k}\simeq 0$-component and it causes *ion-wave generation* from the balance of ion's $\boldsymbol{k}\simeq 0$-component. Our theory also show that, the beam electron can not emit the soliton by itself and any retarded response of Σ_α is required for emission. We obtained also a relation between the $D_{ij}(\boldsymbol{k}, \boldsymbol{v})$, and the electron-vs.-wave collision frequency $\Sigma_\alpha(\boldsymbol{k}, \boldsymbol{v}, \omega)$ as:

$$\mathrm{Re}\,\Sigma_\alpha = y^2 \cdot \frac{D_{ij}}{|\, \boldsymbol{v} - \boldsymbol{v}' \,|^2}\,, \tag{6}$$

where the y has a varue of 0~1. The eq. (6) is a anomalous collision frequency obtained by Tsytovich in qusilinear theory [8], if we exchange our correlational length in velocity space, $|\boldsymbol{v} - \boldsymbol{v}'|$, with $\boldsymbol{v}$.

Figure 5 shows the time sequence between the detected envelope of solitons and the 1MHz component signal of ion waves (or cavitons) obtained by HP-8554L-8552B spectrum-analyzer.

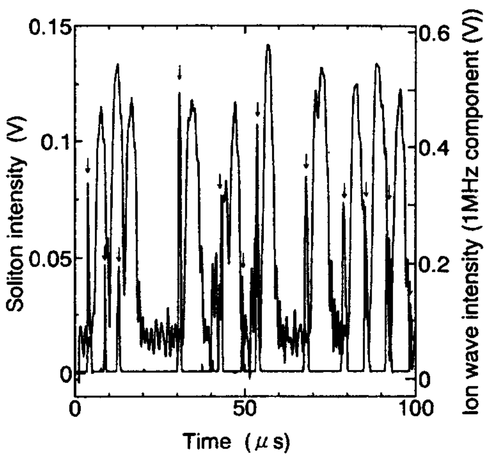

Fig. 5 The strong couplings between the soliton and the ion wave are presented. The pointed peaks shown by the arrows represent envelope solitons and wide peaks are 1MHz component of ion waves. The ion waves are surrounded by dispersive waves whose width are almost same as that of solitons.

Since band width is {\normalsize $\Delta\omega$ = 300KHz, the ion wave is time delayed about $\Delta t \simeq 1.7\mu$s from a relation $\Delta\omega\Delta t \geq$ half-cycle. The pointed peak shown by an arrow represents envelope soliton and the followed wide peaks are 1MHz-component of ion waves. There are also seen that the ion waves are surrounded by a pedestal consisting of dispersive wave whose width is almost same as that of the envelope soliton. Thus the waves would be in the strong coupling state and the results are quite similar to the theory. Our previous paper [9] supports also the situation.

References

[1] I. Mori, Phys. Fluids **28**, 3269 (1985).

[2] I.M. Al'tshul and V.I. Karpman, Sov. Phys. JETP **22**, 361 (1966).

[3] T.H. Dupree, Phys. Fluids **9**, 1773 (1966).

[4] J. Weinstock, Phys. Fluids **12**, 1045 (1969).

[5] M. Kono and Y.H. Ichikawa, Prog. Theor. Phys. **49**, 754 (1973).

[6] C.W. Horton, "*Long time Prediction in Dinamics*", John Wiley p.311 (1983).

[7] I. Mori, T. Morimoto, R. Kawakami and K. Tominaga, to be published in *Nuclear Instrument and Method in Physics Research B* (1999).

[8] V.N. Tsytovitch, "*Nonlinear Effects in Plasmas*" (Trans. by M. Hamberger), p.170 New York-London; Plenum Press (1970).

[9] I. Mori and K. Ohya, Phys. Rev. Lett. **59**, 1825 (1987).